Materials and Structures (2025) 58:337
https://doi.org/10.1617/s11527-025-02836-1

ORIGINAL ARTICLE

Towards enhancing the sustainability of hybrid self-compacting concrete with glass powder, silica slurry, and polyolefin fibers

Khaled Abd-allah Gharib · Amr Aly Gamal-eldin · Mohamed I. Serag · Mohamed O. R. Elhariri · Mohamed A. S. Abd-Elmageed

Received: 12 May 2025 / Revised: 2 August 2025 / Accepted: 13 October 2025 / Published online: 11 November 2025

Abstract Sustainable construction requires advanced materials that minimize environmental damage. This research explores the interaction among fine glass powder (FGP), coarse glass powder (CGP), silica slurry (SS), and polyolefin fibers (PF) in self-compacting concrete (SCC). The optimum combination (15% FGP, 5% SS, 1% PF) improved flow by 17% without reducing strength or causing segregation. Mechanical performance improved significantly: 45.24% enhanced compressive strength, 25.79% increased tensile strength at 28 days, and 80.75% increased flexural strength at 28 days. Durability testing showed 35.7% reduced sorptivity. The microstructure examination (SEM, XRD, stereo microscopy) confirmed a denser structure with fewer voids, increased C-S–H gel formation, and improved pore structure. PF improved post-cracking performance through microcrack bridging, while FGP and SS assisted in making the matrix denser. CGP offered an economic alternative with only a 4.76% loss in strength. The study establishes two sustainable approaches: a high-performance FGP solution and a cost-effective CGP alternative, advancing sustainable construction through effective waste utilization.

Keywords Self-compacting concrete · Fine glass powder · Polyolefin fibers · Sustainable construction

1 Introduction

The construction industry plays an essential role in global environmental impact, contributing significantly to natural resource reduction and carbon emissions. As a response to this issue, sustainable construction practices have gained increasing attention, focusing on the use of eco-friendly materials, waste recycling, and performance optimization to reduce the environmental footprint of concrete production. Self-compacting concrete (SCC), known for its superior flowability and ability to consolidate without vibration, has shown great potential as a solution that supports both construction efficiency and material innovation. This specialized composition enables the seamless incorporation of supplementary cementitious materials and fiber reinforcement, resulting in environmentally sustainable concrete systems while preserving both workability and mechanical performance. The present study explores an innovative hybrid approach that integrates fine glass powder (FGP) and coarse glass powder (CGP) both derived from recycled waste glass along with silica slurry (SS), an industrial by-product rich in reactive silica,

K. A. Gharib (✉) · A. A. Gamal-eldin · M. O. R. Elhariri · M. A. S. Abd-Elmageed
Faculty of Engineering at Shoubra, Benha University, Cairo, Egypt
e-mail: khaled.Gharib@feng.bu.edu.eg

M. I. Serag
Faculty of Engineering, Cairo University, Cairo, Egypt

and polyolefin fibers (PF), a synthetic reinforcement known for its durability and crack-bridging capabilities, into SCC. This incorporation aims to enhance the mechanical and durability performance of SCC while addressing key sustainability goals such as resource minimization, waste recycling, and carbon footprint reduction.

Several studies have confirmed the effectiveness of these materials. Kou and Poon [1] found that incorporating recycled glass aggregate into self-compacting concrete enhanced flowability and passing ability through narrow reinforced areas. This improvement results from two key factors: first, the smooth surface texture of glass particles minimizes friction between particles, promoting easier flow; second, the low water absorption of glass aggregate, compared to natural sand, preserves the water content needed for optimal workability. Liu [2] also reported a 12% increment in slump flow in self-compacting concrete with 15% cement substitution using fine glass powder (FGP), attributed to its relatively low water absorption and spherical particle shape, which improves paste flowability. Ibrahim [3] achieved a 15% gain in 28-day and 22% in 90-day compressive strength using 20% waste (FGP) along with silica fume and fly ash. This enhancement was attributed to the synergistic pozzolanic reaction, where the FGP and silica fume supplied reactive silica that combined with $Ca(OH)_2$ to form additional C-S–H gel. However,

Adaway and Wang [4] Studied the use of recycled glass as a partial replacement for natural sand in concrete and found that replacement levels up to 30% slightly improved compressive strength—by around 9% at 7 days and 6% at 28 days. However, higher replacements beyond 30% led to reductions in strength due to limitations in cement paste availability and increased interfacial voids due to angular particle shape. Khan [5] demonstrated an 18% improvement in strength utilizing 10% fine glass powder combined with 10% silica fume as a replacement for cement, this enhancement due to increased pozzolanic activity and improved filler effect. Dobiszewska et al. [6] showed minimal loss in strength with up to 10% (FGP) replacement at 90 and 180 days, indicating a long-term contribution to the hydration process.

Much of the existing research highlights improvements in durability performance. Ortega et al. [7] found better chloride resistance with 10–30% waste (FGP), decreasing the absorption coefficient by up to 52.6%. This was linked to the denser microstructure resulting from pozzolanic activity and particle packing. Safarizki et al. [8] found enhanced durability through pozzolanic reactions that created more C-S–H, with SEM showing glass particles dispersed in a dense gel matrix. Idir et al. [9] found that the pozzolanic activity of particles under 100 µm exhibited significant pozzolanic activity, which contributed to denser matrix formation. Aliabdo et al. [10] attained 25% improved acid attack resistance and 30% improved freeze–thaw durability with 20% (FGP), which they attributed to the chemical stability of glass and the densification of the matrix through secondary C-S–H gel formation. Mohy et al. [11] achieved a 22% strength increase with 10% FGP and 5% silica fume, explaining that the hybrid use of reactive fillers enhanced both the microstructure and the interfacial transition zone (ITZ). Abo El-Kassem et al. [12] attained 30% improved chloride resistance and 25% reduced permeability with 15% (FGP), This improvement is again associated with pore refinement. Yusuf et al. [13] Showed a 28% increase in compressive strength and a 35% improvement in sulfate resistance with 20% FGP and 10% silica fume. The enhanced chemical resistance was due to reduced calcium hydroxide content and improved microstructure. Tariq et al. [14] set up high-volume (FGP) (up to 40%) improved aggressive environment resistance of self-compacting concrete by 25% without affecting workability, owing to its filler effect and lower alkali-silica reactivity.

Safarizki et al. [15] found that substituting 20% of sand with FGP improved compressive strength and workability by 15% and 10%, respectively. This was related to better particle grading and reduced voids in the mix. Said et al. [16] also showed 25% strength gain and 40% permeability reduction by the use of 3% nano-silica slurry due to improved dispersion and matrix densification. Behnood and Ziari [17] reported that 10% of silica fume achieved 30% residual compressive strength when exposed to 800 °C at 25%, attributing the result to thermally stable hydration products and reduced mass loss.

Concerning fibers, Alberti et al. [18] reported that the addition of 1% polyolefin fibers in SCC improved flexural strength by 40% and toughness by 60%. due to energy absorption capacity and crack-bridging effects and Ponikiewski [19] reported that (PF) resulted in 30% more ductility and 25% better crack control, although compressive strength was reduced by 20% due to lower stiffness.Afroughsabet and Ozbakkaloglu [20] discovered that hybrid fibers (0.75% steel, 0.25% polypropylene) enhanced compressive strength by 35%, splitting tensile strength by 50%, and freeze–thaw resistance by 40%. These improvements are attributed to the combined crack-bridging effect of steel fibers and the ductile energy absorption of polypropylene fibers, leading to better microcrack control and matrix cohesion under cyclic loads. Cifuentes et al. [21] found that 50 mm-long fibers at 0.6%, which can be attributed to their optimal aspect ratio and distribution, allow better energy dissipation and efficient crack-bridging under tensile stress.

Banthia and Sappakittipakor [22] found that 70% improvement in flexural toughness was achieved with hybrid fibers (0.5% steel, 0.15% polyolefin). This improvement was attributed to the synergy between the high modulus of steel fibers and the ductile behavior of polyolefin fibers, which together provided superior crack bridging, delayed crack propagation, and improved energy absorption under flexural loading. Adhikary et al. [23] found that 0.75% polyolefin fibers improved post-cracking behavior by 45%, Resulting from effective crack bridging and better fiber dispersion delaying crack propagation.`Behfarnia and Behravan [24] showed that 0.3% polypropylene fibers improved durability by 30% and reduced permeability by 25%, likely due to void filling and inhibition of microcrack development within the matrix. Alberti et al. [25] showed that the addition of 0.5% polyolefin fibers made structures 35% more bend-resistant and improved crack control by 50%, attributed to better fiber anchorage and crack-bridging effects delaying crack formation. Smirnova et al. [26] noted that 0.1% polyolefin fibers improved freezing and thawing resistance by 40% and decreased shrinkage cracking by 35%, likely because fibers reduce pore Network formation and enhance cohesion under cyclic moisture stresses. Sabri et al. [27] noted that 0.5% polyolefin fibers improved impact resistance by 50% and decreased permeability by 20%, derived from improved energy absorption and refined pore structure resisting external loads.

Building on the insights from previous studies, this research develops and evaluates a set of hybrid SCC mixtures combining multi-grade glass powder, silica slurry, and polyolefin fibers, aiming to optimize both sustainability and performance. A total of 13 SCC mixtures divided into three groups will be assessed in this study. A comprehensive research program is conducted to evaluate both fresh and hardened properties as well as the durability of these new mixtures, while also considering in detail their mechanical performance along with their microstructural features. The testing will be performed using several advanced analytical techniques: Scanning Electron Microscopy (SEM) for microstructural examination, X-ray diffraction (XRD) for phase composition analysis, Stereo microscopy for surface morphology study, and Brunauer–Emmett–Teller (BET) analysis for porosity characteristics. This will allow us to gain a deeper understanding of the mechanisms underlying the performance witnessed in these modified SCC mixtures.

The present study will investigate how combining these materials in concrete influences its structure and overall performance, aiming to establish the foundation for developing environmentally friendly, durable concrete solutions that could significantly reduce environmental impact while enhancing construction methods.

2 Experimental program

2.1 Ordinary portland cement

This is a standard Type I Portland cement that meets ASTM C150 specifications. It achieves a compressive strength of 42.5 MPa in 28 days and a density of 3.15 g/cm^3.

2.2 Fine aggregate

The sand used in the study was from the Nile River basin in Egypt and conformed with ASTM C33. Its physical properties were as follows: specific gravity of 2.6, maximum particle size of 4.75 mm, and water absorption of 1.2%. The particle size distribution was determined according to ASTM C136. The sand gradation curve in Fig. 1 is within the acceptable limits provided by ASTM C33.

2.3 Coarse aggregate

The crushed dolomite used in the study was from Gebel Ataqa quarries in Egypt and conformed with ASTM C33. Its physical properties were as follows:

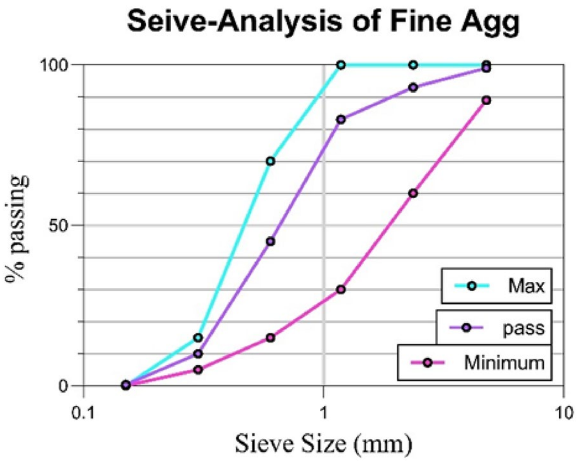

Fig. 1 Particle size distribution curve of the sand

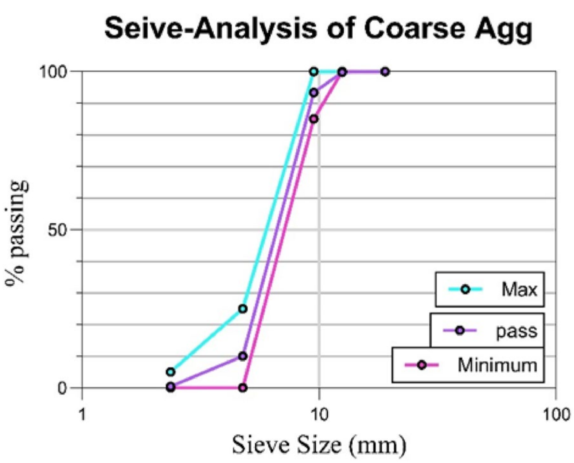

Fig. 2 Particle size distribution curve of the crushed dolomite coarse aggregate

specific gravity of 2.5, maximum particle size of 12.5 mm, and water absorption of 0.5%. The particle size distribution was determined according to ASTM C136. The coarse aggregate gradation curve in Fig. 2 is within the accepted limits.

2.4 Glass powder

Two grades of glass powder were used as a sand replacement in this study. Fine Glass Powder (FGP), produced from high-purity Secorite glass with transparent white color, was ground to 5 µm particle size. Coarse Glass Powder (CGP), produced from ground bottles of soda, was ground to 100 µm. Particle size distribution was examined by Dynamic Light Scattering (DLS) technique. The chemical compositions of both glass powders are provided in Table 1.

2.5 Silica slurry

Concrete mix designs in SCC in this study involved Sika® Fume Slurry (SS), high fine silica fume suspension in water, as an addition of cement to SCC mixtures. The suspension contains active fine silica particles of an average size of about 0.1µm. The product contains 50% solid content and has a 1.38 ± 0.02 specific gravity. The product appears grey and uniform like slurry. The fine particle size of silica offers an immense surface area that supports pozzolanic activity, which in turn can contribute to enhanced strength and life of the concrete. This slurry formulation enhances homogenously distributed performance within the cementitious matrix, thus yielding enhanced microstructure throughout the concrete.

Table 1 Chemical Composition of Glass Powder, cement, and Silica slurry

Compound	Fine Glass %	Coarse Glass %	Cement %	Silica Slurry %
SiO_2	72.22	69.95	20.8	49.8
Na_2O	13.6	15.5	0.22	0.1
CaO	11.5	12.8	63.9	0.03
MgO	0.32	0.85	2.3	0.02
Al_2O_3	1.9	2.15	5.2	0.03
K_2O	0.35	0.45	0.82	0.01
Fe_2O_2	0.07	0.12	3.1	0.02
TiO_2	0.04	0.08	0.26	0.01
SiO_2	–		2.4	0.01
H_2O	–		–	49.95

According to the manufacturer's technical datasheet, the silica slurry contains < 0.10% chloride ions and is hence regarded as being chloride-free. 0.12% sodium equivalent oxide content is indicative of low alkali contribution. The chemical composition of the silica slurry content is given in Table 1.

2.6 Fiber (polyolefin)

Raman spectral analysis (Fig. 3) of polyolefin fiber manufactured by Sika Egypt reveals the vibrational pattern that characterizes high-performance polyolefin fibers for the reinforcement of concrete. In this spectrum, distinct molecular fingerprints can be identified by several key vibrational bands. Major peaks at 2849 cm^{-1} and 2884 cm^{-1} correspond to the symmetric and asymmetric CH_2 stretching modes, respectively, reflecting the basic hydrocarbon chain. The important vibrational modes are also identified at 1438 cm^{-1} for CH_2 bending, 1130 cm^{-1} and 1298 cm^{-1} for C–C skeletal stretching, and 511 cm^{-1} for C–C bending, all indicating a well-ordered molecular architecture. Figure 3 shows spectral features of high resolution and intensity in the region of 2800–3000 cm^{-1}, which is indicative of optimum crystallinity and molecular orientation. The absence of any additional vibrational modes confirms the compositional purity of the material, therefore confirming a precisely engineered polyolefin system with both a polyethylene and polypropylene component. These spectroscopic features are consistent with superior mechanical properties like high tensile strength, low creep behavior, and excellent chemical stability, for which concrete reinforcement applications would show a particular need. The observed molecular organization and structural features align precisely with the requirements for advanced construction materials, especially in applications that require high durability, effective shrinkage control, and improved crack resistance in civil engineering structures.

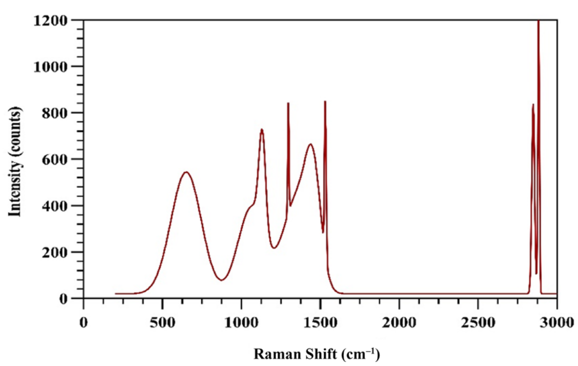

Fig. 3 Raman Spectrum of Polyolefin Fiber

2.7 Chemical admixtures

Sika Visco Flow® 102: This high-performance concrete admixture enhances workability and maintains slump using advanced polycarboxylate polymer technology. It improves plasticity and extends slump retention without additional cost. The admixture has a reddish liquid appearance and a specific gravity of 1.05 g/cm^3.

2.8 Mix characteristics and specimen dimensions

The self-compacting concrete (SCC) was prepared and tested by some procedures. Fresh properties of the mixes made with Portland cement, aggregates, glass powder, polyolefin fibers, and other dry ingredients were determined by tests such as slump flow, L-box, J-ring, and GTM after mixing the raw materials. Mix proportions used for tests were as per values outlined in Table 2: Mix Design Proportions for Self-Compacting Concrete Mixtures. Then, the concrete was cast in moulds, prepared with much care, in the following sizes: cubes (100 × 100 × 100 mm) for compressive strength tests; cylinders (100 mm diameter × 200 mm height) for splitting tensile strength tests; and prism beams (70 * 140 mm, L = 500 mm) for flexural strength tests, ensuring accuracy for representation in subsequent testing.

2.9 Casting and curing specimens

This paper presents an experimental study that involves a great deal of preparation and exhaustive tests of the self-compacting concrete mixtures according to the methodologies given for batching and mixing their constituent materials. Immediately after adding water and chemical admixture by a metering pump in a well-defined process of 6-min mixing to ensure the homogeneity of the mix before mold preparation, tests characterizing all fresh properties will be conducted before the mixture casting. After verification, the concrete underwent systematic casting procedures followed by surface finishing operations

Table 2 Mix design proportions for Self-Compacting Concrete (SCC) mixtures

No of Mix	No Of Label	Cement kg/m^3	Fine Agg kg/m^3	CoarseAgg kg/m^3	water kg/m^3	Glass Powder kg/m^3	Slurry kg/m^3	Fiber kg/m^3	Vma kg/m^3
S-CL		450	859.12	966.5	175.5	0.0	–	–	11.3
Group1	S-0.6%FP	450	859.12	966.5	175.5	–	–	2.7	11.3
	S-1%FP	450	859.12	966.5	175.5	–	–	4.5	11.3
	S-1.5%FP	450	859.12	966.5	175.5	–	–	6.8	11.3
	S- 2%FP	450	859.12	966.5	175.5	–	–	9.0	11.3
Group2	S-FGP5% + SS 5% + FP1%	427.5	790.40	966.5	166.7	41.6	22.5	4.5	11.3
	S-FGP10% + SS5% + FP1%	427.5	748.80	966.5	166.7	83.2	22.5	4.5	11.3
	S-FGP15% + SS5% + FP1%	427.5	707.20	966.5	166.7	124.8	22.5	4.5	11.3
	S-FGP20% + SS5% + FP1%	427.5	665.60	966.5	166.7	166.4	22.5	4.5	11.3
Group3	S-CGP5%	450.0	816.12	966.5	175.5	41.6	–	–	11.3
	S-CGP10%	450.0	773.21	966.5	175.5	83.2	–	–	11.3
	S-CGP15%	450.0	730.25	966.5	175.5	124.8	–	–	11.3
	S-CGP20%	450.0	687.30	966.5	175.5	166.4	–	–	11.3

and the implementation of appropriate curing measures. The curing protocol consisted of a two-phase curing approach: controlled curing for the first 24 h followed by standard curing conditions according to ASTM C31 for specimens tested at ages of 7, 28, 56, and 90 days.

2.10 Testing methods

2.10.1 Fresh properties

The fresh properties of SCC mixtures were evaluated using four Internationally recognized standard methods: slump flow testing according to EN 12350–8 [28], which enables assessment of flowability and filling capacity; J-Ring testing according to EN 12350–12 [29], used for evaluating the mixture's ability to pass through confined spaces; L-Box testing according to EN 12350–10 [30], which analyzes flow behavior around reinforcement bars; and Grading Test Method (GTM) according to EN 12350–11 [31], which measures resistance to dynamic segregation. These test methods have provided crucial data regarding the mixtures' workability, cohesion, and stability, which is fundamental for designing optimized mixes that meet contemporary engineering and construction requirements.

2.10.2 Hardened properties

The mechanical properties of the SCC mixtures were tested according to standardized tests provided by ASTM. Resistance of mixtures to axial loads was determined in compressive strength tests (Fig. 4-a), according to the requirements of ASTM C39. In split cylinder tests, Fig. 4-b, tensile strength under splitting was investigated based on the indications of ASTM C496, to material resistance under tension. Flexural strength was measured using a four-point loading setup, where each beam was simply supported at both ends and symmetrically loaded at two points located at one-third of the span length, as shown in Fig. 4-c. This setup conforms to the procedure outlined in ASTM C78, which defines the standard method for evaluating flexural performance in concrete. Therefore, these tests will offer, in detail, how SCC behaves mechanically.

2.10.3 Durability characteristics

Water absorption properties of hardened SCC were determined according to ASTM standards. The sorptivity testing was conducted by ASTM C1585 [32], which measures the rate of capillary water absorption and is used to evaluate some properties of the pore structure of concrete, including how supplementary cementitious materials can enhance the microstructure. Higher values of sorptivity indicate poorer durability since concrete is more prone to damage. The water absorption test, ASTM C642 [33], provides an indication of the porosity of concrete and resistance to penetration. The less

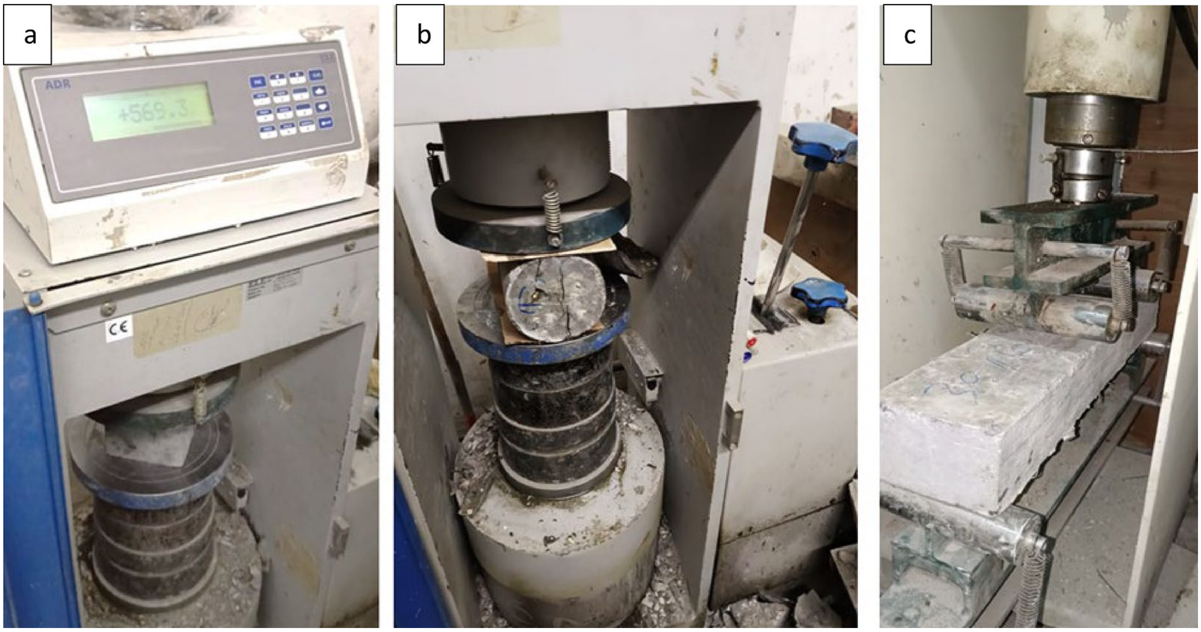

Fig. 4 Testing equipment for compressive (**a**), splitting tensile (**b**), and flexural (**c**) strength of Self-Compacting Concrete

absorption, the lower the susceptibility to deterioration; hence, the higher the long-term durability.

2.10.4 Microstructure

Several advanced techniques characterized the microstructure of SCC. SEM was carried out on a JEOL JSM-7600F field emission SEM equipped with energy-dispersive X-ray spectroscopy (EDS) for elemental analysis. Stereo imaging, to obtain three-dimensional surface topography, was performed on a Nikon SMZ1500 stereomicroscope with a digital camera. XRD analysis was carried out using a Bruker D8 Discover diffractometer with Cu Kα radiation, required for the identification of crystalline phases. The particle size distribution and consistency, with a high degree of accuracy, were measured using dynamic light scattering data collected on a Zetasizer from Malvern Instruments Ltd., UK. For surface area and porosity analysis: BET surface area was measured and the volume was determined using a Nova Touch 2X gas sorption analyzer by Quanta Chrome Instruments. The nitrogen gas adsorption–desorption isotherms were used in this process to get insights regarding the surface features and pore structure of the samples. This all-inclusive approach has given a deep understanding of the structure and properties of the SCC mixture, hence elucidating how its components interact and influence overall performance at a larger scale.

3 Results and discussion

3.1 Fresh concrete properties

A comprehensive experimental program was carried out to evaluate the fresh properties of SCC mixtures through a group of standard tests. Table 3 presents experimental results obtained from three groups of concrete mixtures, each designed to study some variables. Group 1 considered fiber content ratios ranging from 0.6% to 2%. Group 2 investigated fine glass powder contents ranging from 5 to 20% at constant parameters of 5% silica slurry and 1% fiber content. Group 3 examined the coarse glass powder substitution from 5 to 20%. A control mix (S-CL) was established as the reference baseline for comparison. In each mixture, five critical fresh properties were measured as slump flow diameter, D mm, and T500

Table 3 Fresh properties of SCC mixtures with varying glass powder, silica slurry content, and polyolefin fiber content

NO OF GROUP	NO OF MIX	slump flow D mm	T500 sec	l-box h2/h1 mm	Jring test mm	GTM-test %
S-CL		555	6	0.8	5	6
Group1	S-0.6%FP	550	6	0.7	25	3
	S-1%FP	547	8	0.65	30	6
	S-1.5%FP	520	12	0.5	35	12
	S- 2%FP	480	20	0.4	35	18
Group2	S-FGP- 5% + SS5% + FP1%	540	7	0.7	6	10
	S-FGP-10% + SS5% + FP1%	560	5	0.78	8	12
	S-FGP -15% + SS5% + FP1%	610	5	0.8	15	15
	S-FGP- 20% + SS5% + FP1%	650	4	0.84	18	18
Group3	S-CGP5%	540	10	0.73	6	6
	S- CGP 10%	520	16	0.68	12	4
	S- CGP 15%	480	25	0.63	15	4
	S- CGP 20%	450	30	0.6	20	3

According to EN 12350, the acceptance criteria for SCC fresh properties are: slump flow (SF1: 550–650 mm, SF2: 660–750 mm, SF3: 760–850 mm), L-box passing ratio (h2/h1) ≥ 0.8, J-Ring blocking step (PJ1: ≤ 10 mm, PJ2: ≤ 20 mm) with maximum difference from slump flow ≤ 50 mm, and GTM segregation resistance (SR1: ≤ 20%, SR2: ≤ 15%)

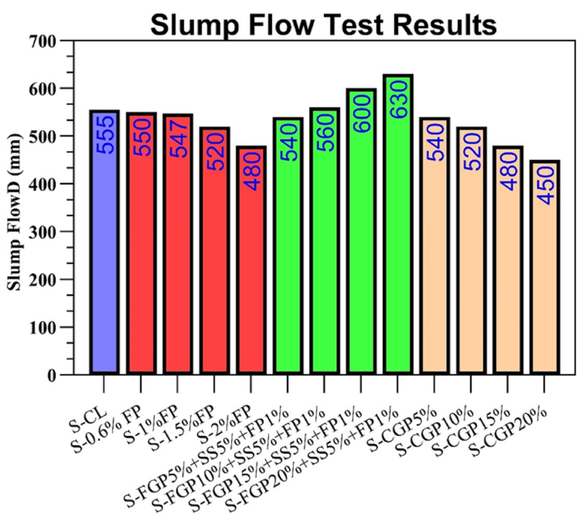

Fig. 5 Slump flow test results for different mix designs

time (seconds) to measure the time required for the concrete to flow to a 500 mm spread diameter indicating flowability, passing ability through L-box h2/h1, J-ring flow in mm, and GTM segregation resistance %.

3.1.1 *Slump flow test*

The present research discusses the effect of additives on SCC flowability, as considered by slump flow diameter. The relevant slump flow diameters are presented in Table 3 and Fig. 5. This study includes the following mixed categories: Group1-FP only, Group2-combinations of FGP + SS + FP, and Group3-CGP content. In Group 1, the effect of FP was to decrease flowability inversely, with slump flow falling from 550mm at 0.6% to 480mm at 2% content, giving a slump flow reduction of 12.7%. It is, however, critical to note that the principal role of FP is to decrease segregation in very flowable mixes and workability reduction is a secondary effect. The combination of FGP, SS, and FP resulted in a remarkable workability enhancement in Group 2. Slump flow improved from 540mm for concrete containing 5% FGP to 650mm for that containing 20% FGP (all containing 5% SS and 1% FP), corresponding to an improvement of 17%. This great enhancement can be attributed to the lubricating effect of SS and the superior particle packing facilitated by fine glass particles. On the contrary, in Group 3, with the increase of CGP content, workability showed negative influence and slump flow value decreased from 540 mm at 5% CGP to 450mm at 20% CGP, an 18.7% reduction.

This severe deterioration is arguably because of the angular shape of the coarse glass particles, which would increase the internal friction. The best blend in Group 2 was with 20% FGP, 5% SS, and 1% FP, and it had a slump flow 17% higher than that of the control mix. This research emphasizes the need to balance flowability against other critical properties, especially resistance to segregation.

3.1.2 J-Ring, L-Box Test, and T500

Based on the rheological tests (Table 3), there are some correlations between additives and fresh SCC properties. Control mix (S-CL) was satisfactory with T500 = 6 s and L-box ratio = 0.8. In Group 1, 1% polyolefin fibers (FP) were optimal, providing T500 = 8 s and L-box ratio = 0.65. This moderate rise in plastic viscosity is beneficial to suspend fibers without a drastic loss of flowability. At 2% FP, T500 increased to 20 s (233% increase), reflecting very high viscosity due to fiber interference and loss of workability. Group 2 (Hybrid Mineral Additions), containing 1% FP exhibited synergy. The best mix (10% fine glass powder + 5% SS + 1% FP) reduced T500 to 5 s with very good passing ability (L-box ratio = 0.78). This was achieved by: (i) FGP spherical particles minimizing friction, (ii) SS micro-filling effect minimizing water demand, and (iii) cohesive matrix stabilizing fiber networks without disrupting rheology. Group 3 with Coarse Glass Powder (5–20%) had a greater T500 (10–30 s) as CGP angular particles increased friction. Mixture passing ability was satisfactory (L-box ratios > 0.6) despite high viscosity due to CGP's well-balanced particle size distribution. The ideal combination (10% FGP + 5% SS + 1% FP) realized the optimum T500 (5 s) and met SCC requirements through complementary components: FP stabilizes without over-viscosity, FGP improves flow through friction reduction, and SS matrix optimizes through micro-filling, yielding workable, stable, homogeneous SCC.

3.1.3 GTM Test

Based on Table 3 and Fig. 6, the segregation test (GTM) results show complex interactions between additives affecting SCC mixture stability against ASTM15% critical limit. The control mix (S-CL) provided a reference with 6% GTM, which was

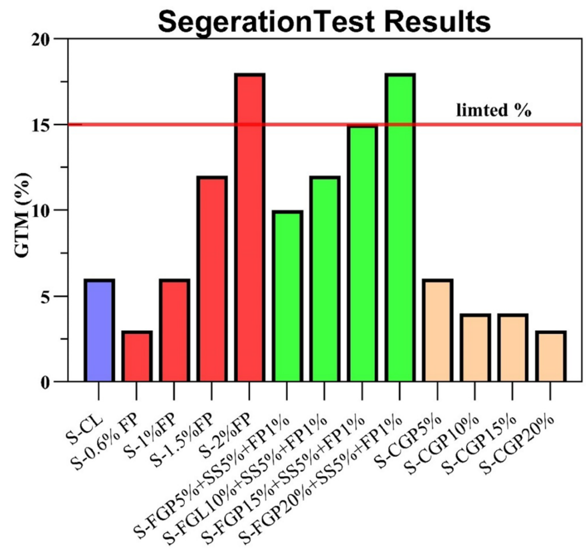

Fig. 6 Segregation Test Results for various concrete mix designs

extremely stable because of particle distribution and water balance. In Group 1, 1% polyolefin fiber (FP) achieved peak performance with 6% GTM because of effective fiber dispersion and matrix reinforcement. Increasing up to 2% FP raised GTM to 18% due to fiber agglomeration-induced matrix inhomogeneities, reflecting the critical balance of fiber content. Group 2 investigated mineral additives at optimal fiber content, and the optimal was 10% FGP + 5% SS + 1% FP (12% GTM). This was because: (i) spherical FGP particles increase packing density, (ii) micro-filling by silica slurry filling up voids, and (iii) optimal fiber content stabilizes the matrix, demonstrating how mineral additions can mitigate fiber-induced segregation risks. Group 3 with Coarse Glass Powder (5–20%) exhibited improved segregation resistance with increasing contents of CGP, GTM values lowering from 6 to 3%. This improvement results from CGP's particle morphology causing interlocking effects between aggregates and filling pores between them, while its angular particles increase internal friction to reduce particle separation. Conversely, even though CGP blends produced the lowest GTM values, Group 2 mixture (10% FGP + 5% SS + 1% FP) possessed the best workability-stability mixture and therefore is most suitable for construction purposes that require both characteristics.

3.2 Hardened concrete properties

3.2.1 Compressive strength

Mechanical properties of self-compacting concrete (SCC) mixes with various additives: the study indicated varied performance patterns among three additive groups. Group 1, shown in Fig. 7a, demonstrated moderate but consistent compressive strength improvements through polyolefin fiber incorporation. The S-1% FP mixture achieved optimal results, reaching 29.3 N/mm^2 at 7 days and 47 N/mm^2 at 90 days, representing increases of 8.5% and 11.9% over the control mix. This improvement is due to the fiber's capacity to bridge microcracks and distribute stress throughout the concrete matrix. Group 2, represented in Fig. 7b, showed the most substantial performance increases through hybrid combinations of fine glass powder (FGP), silica slurry (SS), and polyolefin fiber (FP). The S-FGP15% + SS5% + FP1% combination obtained remarkable results, with compressive strength values of 37.4 N/mm^2 at 7 days (38.5% increase) and 61 N/mm^2 at 90 days (45.2% increase). This superior performance results from

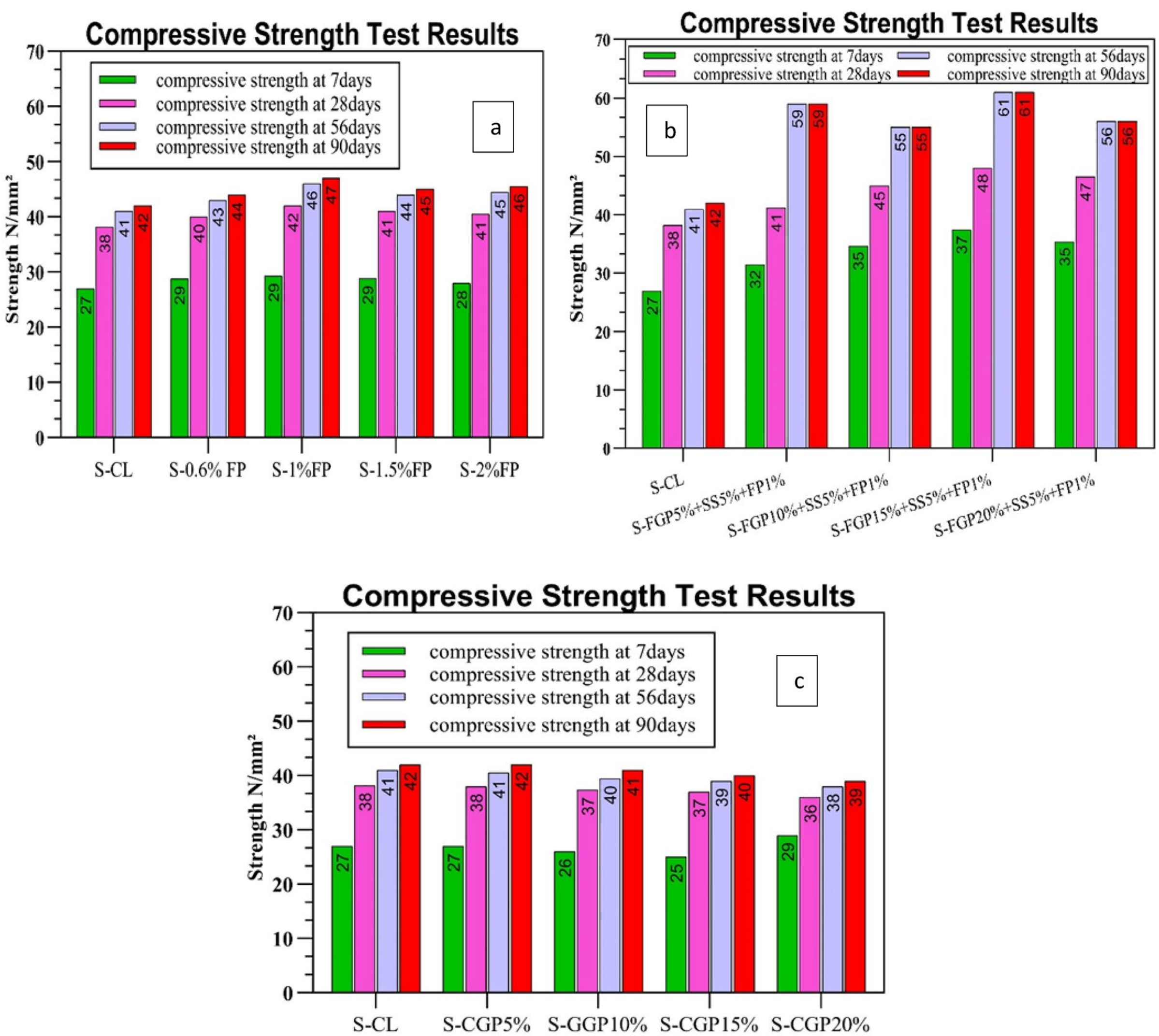

Fig. 7 Comparative analysis of compressive strength development for various concrete mix designs across four distinct groups: (**a**) Group1, (**b**) Group2, and (**c**) Group3

complementary mechanisms: fine glass powder improves the concrete matrix physically and chemically. The glass particles create favorable conditions for further hydration through moisture retention and gradual release while preventing microstructural degradation. Group 3, illustrated in Fig. 7c, showed slight strength decreases as coarse glass powder (CGP) content increased, with 90-day values declining from 42 N/mm^2 at 5% CGP to 39 N/mm^2 at 20% CGP. This performance disparity between fine and coarse glass powder stems from their physical characteristics. Fine glass powder, made by grinding tempered glass into fine particles, has a larger surface area for pozzolanic reaction. Conversely, coarse glass powder, produced from soda-lime glass waste and crushed to larger sizes, results in weaker interfacial zones and increased porosity. Microstructural investigations through advanced techniques will be conducted to comprehensively validate these mechanical testing results, providing deeper insights into the material's internal structural dynamics. Among all tested mixtures, The S-FGP15% + SS5% + FP1% mixture from Group 2 performed optimally due to the synergistic combination of fine glass powder's pozzolanic activity, silica slurry's early strength augmentation, and crack-bridging capabilities of polyolefin fiber.

3.2.2 Tensile and flexural strength

Based on a detailed analysis of tensile and flexural strength properties of Self-Compacting Concrete (SCC), there was a significant performance improvement after 28-day curing. Group 1 (Fig. 8a): Effects of Polyolefin Fiber: The experimental investigation revealed that the inclusion of polyolefin fibers showed a significant influence on mechanical behavior. For the best 1% fiber ratio (S-1%FP), the concrete achieved peak performance with tensile strength of 4 N/mm^2 (25.8% increase compared to control) and flexural strength of 8 N/mm^2 (100% increase compared to control). The primary mechanism of reinforcement identified is the formation of a three-dimensional fiber network in the whole cementitious matrix. This microstructural enhancement is responsible for the observed doubling of flexural strength in comparison to the control mix. The test also showed that the relationship between fiber content and mechanical behavior is non-linear, with 2% content causing fiber cluster, which created matrix discontinuities, while 0.6% content was insufficient for the matrix to be optimally reinforced. The fibers operate as micro-reinforcement in expected fracture zones, successfully confining microcracks before they grow into macroscopic fractures.

Group 2 (Fig. 8b): Complementary Hybrid Mixtures: The mechanical tests revealed that hybrid combinations had a higher developed strength enhancement. The optimal mix S-FGP15% + SS5% + FP1% performed better with 4 N/mm^2 tensile (25.8% increase compared to control) and 7.23 N/mm^2 flexural strength (80.8% increase compared to control). The testing showed three mechanisms of reinforcement operating synergistically: the fine glass powder as a micro-filler, which optimizes the particle packing density; the silica slurry contributing to strength development by pozzolanic reactions that mature; and the polyolefin fibers supplying superior tensile and flexural strength. The synergistic action produced a dense, well-bonded matrix with enhanced crack resistance. The results indicate that the resultant composite materials achieve performances higher than their contributions for each of the constituent materials.

Group 3 (Fig. 8c): Coarse Glass Powder Effect: Experiments on the addition of coarse glass powder yielded significant findings of particle size influence on mechanical properties. The testing showed that starting with S-CGP5% (tensile: 3.15 N/mm^2 [1% decrease compared to control], flexural: 3.95 N/mm^2 [1.3% decrease compared to control]), increasing CGP content resulted in progressive strength deterioration, reaching minimum values at 20% content (tensile: 2.97 N/mm^2 [6.6% decrease compared to control], flexural: 3.68 N/mm^2 [8% decrease compared to control]). The analysis indicates that this decline stems from fundamentally different mechanisms than those observed in Groups 1 and 2. The coarse glass particles form weak interfacial transition zones, effectively inducing microstructural discontinuities in the concrete matrix. Unlike the fine glass powder of Group 2, these coarse particles showed no significant pozzolanic activity but instead behaved as inert inclusions that interfere with matrix continuity.

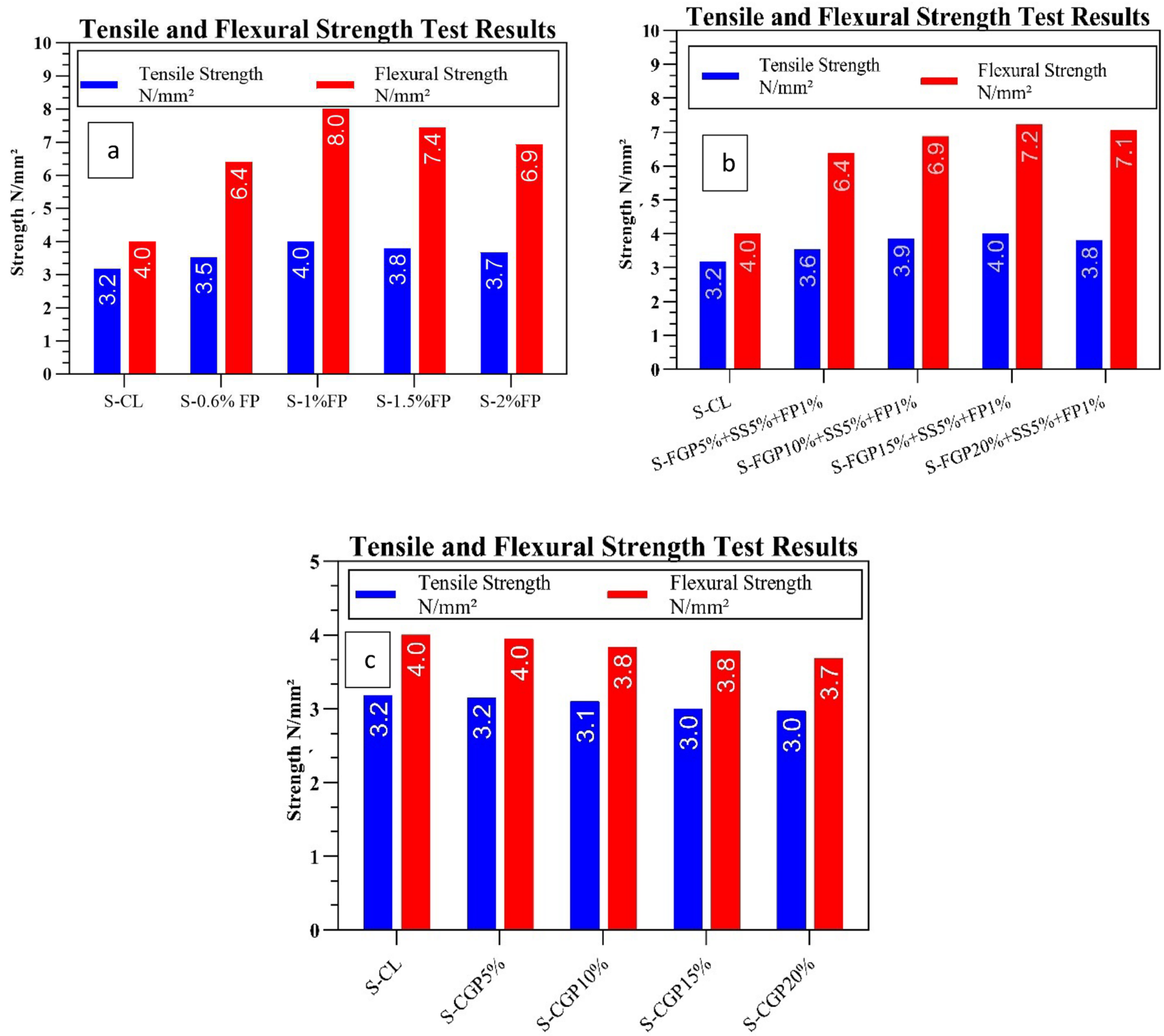

Fig. 8 Comparison of flexural and splitting tensile strength development across different mix designs: (**a**) Group1, (**b**) Group2, and (**c**) Group3

3.2.3 Water absorption

This study investigated the water absorption characteristics of optimum Self-Compacting Concrete (SCC) mixes as given in Fig. 9. In Group 1, different dosages of polyolefin fibers (0.6%, 1%, 1%, 1.5%, and 2%) were tried and compared with S-1%FP as the optimum mix. Notably, this composite retained water absorption (Δmass ≈ 39.5 g) almost like the control composite (Δmass ≈ 39 g), indicating that the well-dispersed fibers at optimum content retain the integrity of the matrix without providing extra channels for water penetration. In Group 2, the hybrid composite S-FGP15% + SS5% + FP1% containing fine glass powder, silica slurry, and polyolefin fibers showed slightly higher water absorption (Δmass ≈ 40 g) compared to the control. This 2.56% increase is particularly noteworthy given the mix's high content of fine materials. Theoretically, the silica slurry, with its high specific surface area, and fine glass powder should enhance matrix density through pozzolanic reactions and improved particle packing. However, SEM analysis showed that although these materials formed an extremely dense matrix with very few visible voids,

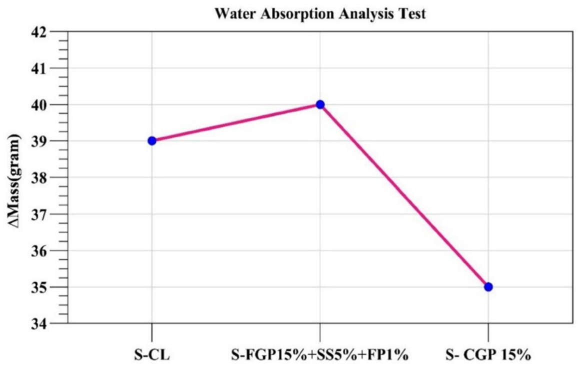

Fig. 9 Comparison of water absorption results for SCC mixtures

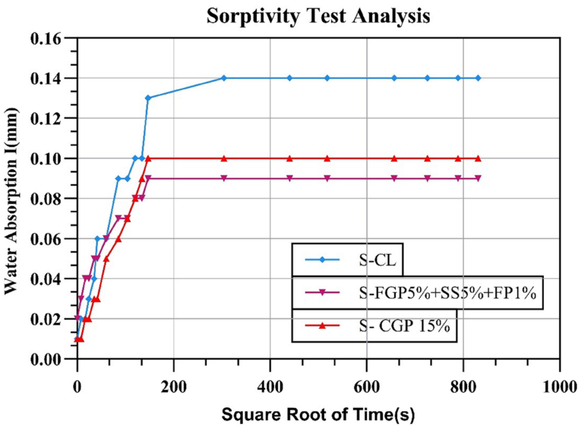

Fig. 10 Comparison of water absorption results for SCC mixtures

the addition of 1% polyolefin fibers created microscopic channels at the fiber-matrix interfaces that formed a network that allowed water to move through the otherwise dense matrix. This finding demonstrates how fiber inclusion can impact water transport mechanisms even in a well-densified concrete matrix. In Group 3, different percentages of coarse glass powder (5–20%) were investigated. S-CGP-15% exhibited the highest water resistance and lowest absorption (Δmass ≈ 35 g), a 10.26% reduction compared to control. Such enhancement is attributed to the large glass particles, which served as barriers blocking the pathways for water penetration. However, SEM analysis shows micro-cracks and weak interfacial zones between glass particles and cement paste; hence, improvement in water resistance may come at the expense of reduced mechanical performance. The main benefit of coarse glass powder is economic viability and environmental sustainability as a readily available recycled material, especially from waste beverage bottles requiring minimal processing. These results have brought into light the complex balance in SCC development between durability, mechanical properties, cost-effectiveness, and sustainability, emphasizing the need for mixed design optimization based on specific performance requirements.

3.2.4 Sorptivity

The experimental examination of the sorptivity coefficient (I), which was obtained from the capillary water absorption testing and presented in Fig. 10, revealed significant performance differences among SCC mixture groups. In Group 1, 1% polyolefin fiber addition (S-1%FP) showed performance equality with the control mixture, confirming that well-dispersed fiber reinforcement maintains matrix integrity without compromising capillary absorption resistance. Notably, the Group 2 ternary blend (S-FGP5% + SS5% + FP1%) produced an improved sorptivity coefficient of 0.09 mm compared to 0.14 mm for the control, which is an improvement of 35.7%. While polyolefin fibers provided additional water absorption pathways through fiber-matrix interfaces, it was effectively neutralized by the combined effect of fine glass powder's pore refinement and enhanced silica slurry's pozzolanic activity. Group 3 studies showed remarkable results, with coarse glass powder (S-CGP15%) yielding a sorptivity coefficient of 0.10 mm—28.6% better than the control mix. This is because the large glass particles create long tortuous paths that force the water to follow longer and more complex paths through the matrix. The mechanism creates discontinuous regions that disrupt potential continuous capillary channels, thereby reducing overall water absorption more effectively than with fine particle systems. This is also corroborated by time-dependent absorption data that demonstrates controlled water ingress behavior with improved tortuosity changes in the pore structure. 15% was determined to be the optimum fine and coarse glass powder content, with coarse particles being more durable to water than fine material pore refinement systems. These findings provide valuable direction for the performance and economic tradeoff in sustainable SCC development, refuting conventional wisdom regarding particle size effects on impermeability and presenting fresh approaches to improving the durability design of concrete.

3.3 Microstructural analysis

3.3.1 Scanning electron microscopy (SEM)

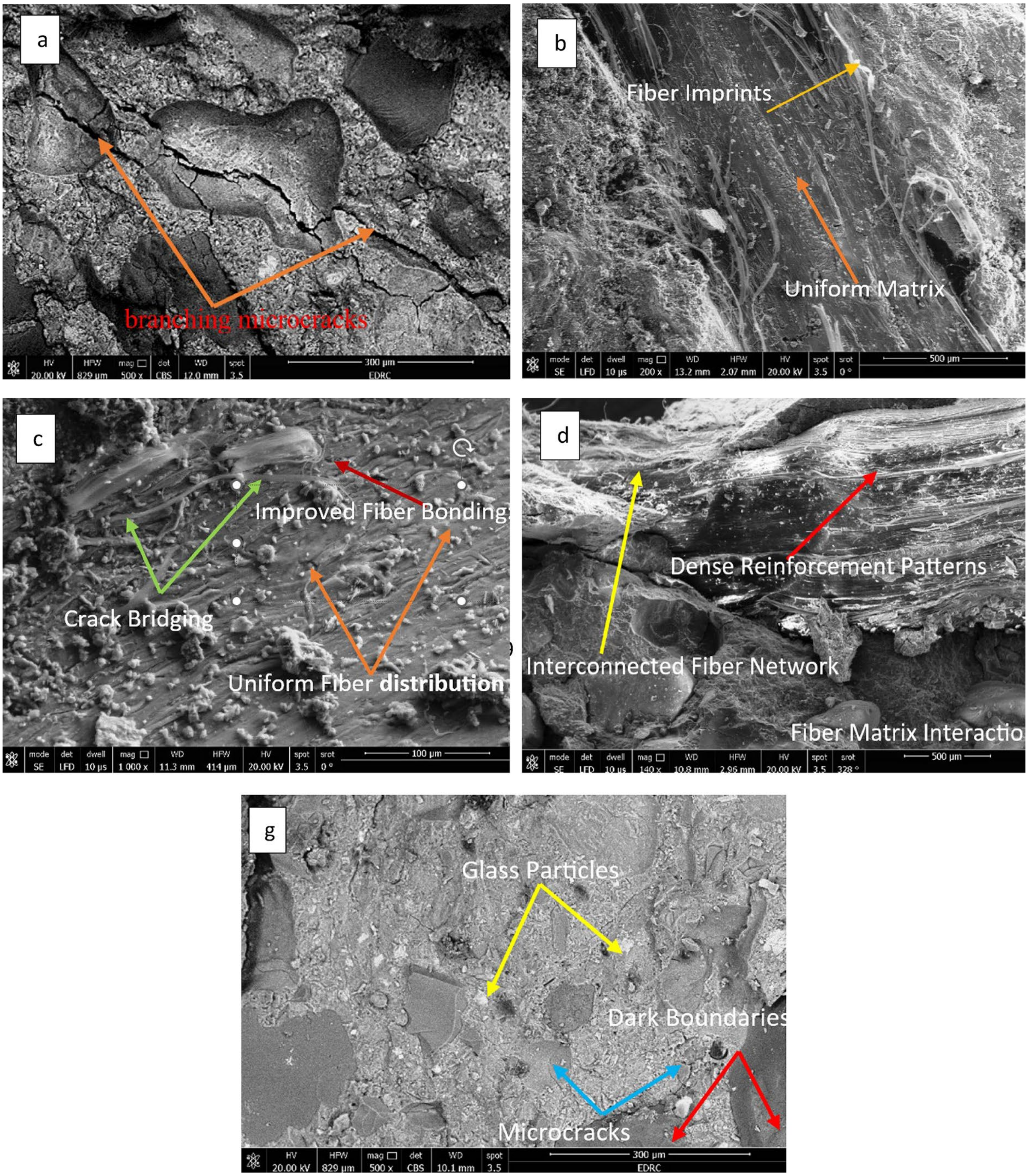

Fig. 11 SEM images of concrete mixtures with various supplementary materials: (**a**) control, (**b**) S-0.6%FP, (**c**) S-1%FP, (**d**) S-1.5% FP, (**e**) S-2%FP, (**f**) S-FGP15% + SS5% + FP1% and (g) S-CGP15%

The microstructural development in concrete mixtures studied by SEM analysis progresses continuously from the control sample shown in Fig. 11a, which exhibits the typical Portland cement structure with clearly visible, coarse, branching microcracks traversing the surface of the concrete, evidence of inherent brittleness of unreinforced concrete. The 0.6% fiber mixture, shown in Fig. 11b, is characterized by a relatively uniform matrix showing distinct fiber influences with minimal matrix-fiber interaction. In comparison, at 1% fiber content, Fig. 11c, the fibers appear uniformly distributed with clear crack-bridging mechanisms and improved fiber-matrix interfacial bonding. The improvement occurs. in the 1.5% specimen (Fig. 11d), revealing an interconnected fiber network creating denser reinforcement patterns, though, at 2% fiber content (Fig. 11e), evident fiber clustering emerges with dense bundles disrupting the surrounding matrix visible in the surface structure. The superior microstructural refinement becomes evident in the optimized mixture of Group 2 (S-FGP15% + SS5% + FP1%), as shown in Fig. 11f, where 15% fine glass powder, 5% silica slurry, and 1% polyolefin fiber together yield an exceptionally dense and uniform microstructure. Fine glass particles can be seen as bright, light-grey angular shapes distributed uniformly in the darker grey C-S–H matrix. The C-S–H regions are distinguishable as main grey areas showing a typical dense and compact texture. The ultrafine silica particles contribute to a very smooth surface appearance, reflecting optimal particle packing and thorough material integration. Within Group 3, the SEM micrograph Fig. 11g for mixture S-CGP15% demonstrates significant bright, angular coarse glass particles that contrast highly against the surrounding cement matrix of relative darkness. The microstructural analysis shows considerable evidence of poor particle integration by the following three main features: significant dark boundary areas surrounding each coarse glass particle, a network of microcracks emanating from the particle interface into the matrix, appearing as dark lines, and significant voids, appearing as dark areas around the particles. The appearance of these structural flaws leads to weakened interfacial zones, explaining the observed degradation of mechanical performance. Compared with the refined microstructure of Group 2, this shows the important role of proper particle size optimization and material combinations in achieving improved matrix densification and enhanced concrete performance due to superior interfacial bonding.

3.3.2 Stereo microscopic

Stereomicroscopic examination, a high-resolution surface analysis technique, was employed to investigate the morphological characteristics of various concrete mixtures, revealing the crucial relationship between composition and microstructural development. The investigation was conducted across three distinct groups to evaluate different aspects of material integration and their effects on mechanical performance. The control specimen (Fig. 12a) exhibited a typical Portland cement matrix characterized by visible microcracks, unreacted particles, and inherent brittleness, reflecting poor interfacial bonding and hence inferior mechanical properties. Group 1 analysis demonstrated the significant influence of fiber content variations on concrete microstructure. At 0.6% polyolefin fiber content (S-0.6% FP) (Fig. 12b), the matrix exhibited moderate fiber restriction with limited fiber-matrix interaction and insufficient provision contribution to crack resistance or mechanical enhancement. The optimal case was observed at 1% content (S-1% FP) (Fig. 12c), featuring homogeneous dispersion and uniform distribution that caused effective crack-bridging mechanisms, thereby improving interfacial bonding and improving mechanical performance. However, higher fiber contents showed negative, with 1.5% content (S-1.5% FP) (Fig. 12d) showing signs of matrix clustering and dense fiber networks that reduced overall uniformity, while 2% content (S-2% FP) (Fig. 12e) led to excessive fiber clustering and bundle formation, disrupting matrix continuity and developing weak zones. Group 2(Fig. 12f) shows the impact of optimally incorporated materials through the incorporation of fine glass powder, silica slurry, and polyolefin fibers (S-FGP15% + SS5% + FP1%). This composition shows dense, homogeneous morphology with well-distributed bright, angular fine glass particles in compact C-S–H regions, visible as light gray to white dense zones. The silica slurry component efficiently refined the pore structure of dark gray smooth zones, reducing interfacial transition zones and Improving matrix cohesion. This optimized mixture achieved Superior density and remaining mechanical performance through combined crack-bridging capability

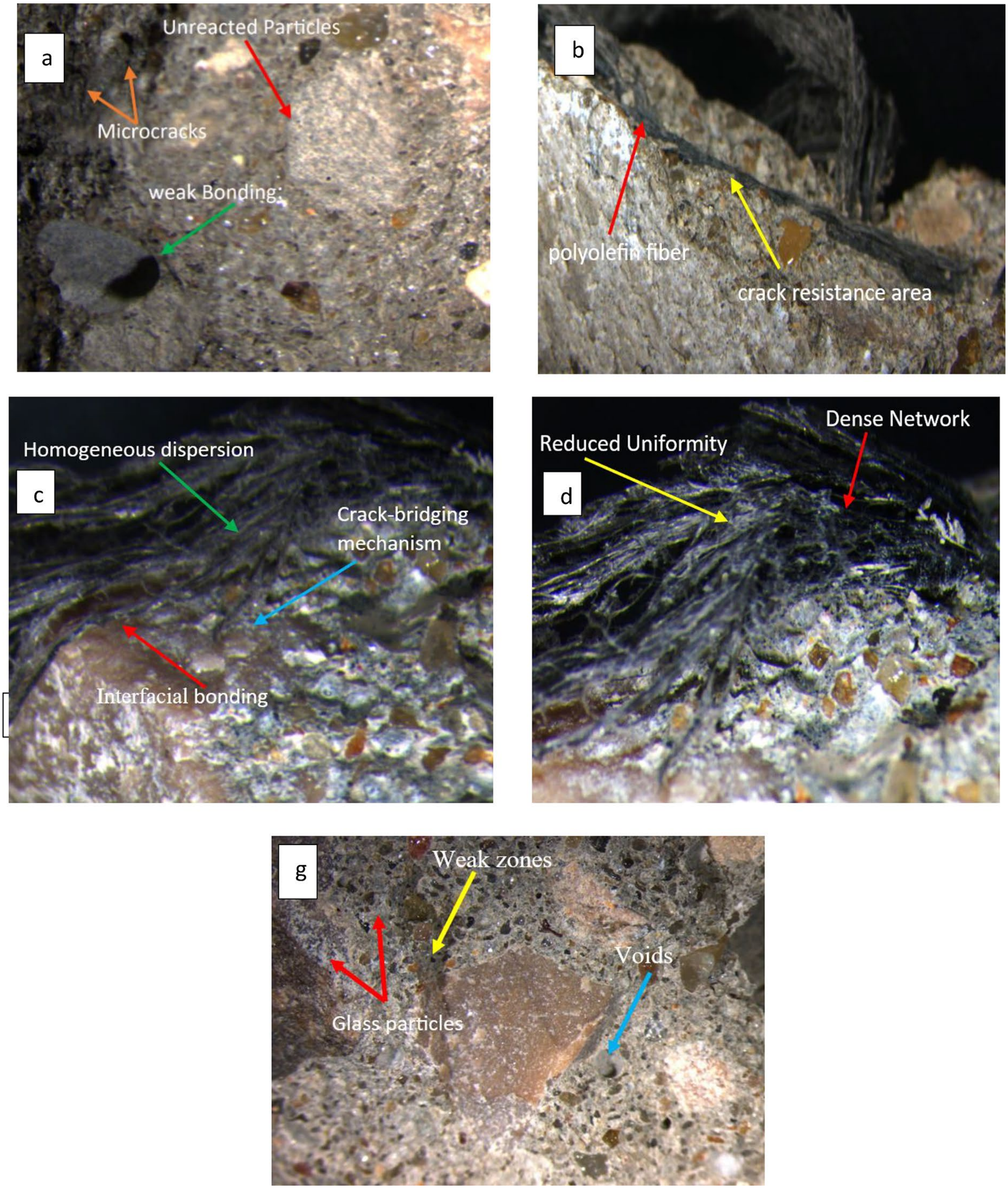

Fig. 12 Stereo images of concrete mixtures with various supplementary materials: (**a**) control, (**b**) S-0.6%FP, (**c**) S-1%FP, (**d**) S-1.5% FP, (**e**) S-2%FP, (**f**) S-FGP15% + SS5% + FP1% and (**g**) S-CGP15%

and stress redistribution within the matrix. Group 3 (S-CGP15%) (Fig. 12g) highlighted the negative effects of coarse glass particle incorporation, characterized by dominant bright, angular particles with significant dark boundary areas and interface-emanating microcracks. The reality of voids near particles weakened the matrix and compromised interfacial bonding, leading to structural defects that disrupted matrix continuity and significantly deteriorated mechanical performance. These findings highlight the crucial role of particle size refinement and suitable material optimization in achieving increased concrete composite performance.

3.3.3 X-ray diffraction (XRD)

A study was conducted on optimal mixtures with pozzolanic reactions that required further clarification and detailed investigation. In the control mixture (S-CL, Fig. 13a), the XRD pattern exhibited dominant crystalline phases produced by primarily from the raw sand rather than hydration products. Orthoclase was identified as the major phase (57.10%), with its most intense diffraction peak at 2θ = 30.7°, along with secondary reflections at 2θ = 23.4° and 25.6°, matching to the feldspar structure of natural sand. Quartz was present at 27.9%, indicated by its strongest reflection at 2θ = 26.7° and a secondary peak at 2θ = 20.8°, reflecting unreacted silica content. Calcite (10.2%) was detected with its main diagnostic peak at 2θ = 29.4° and an additional reflection at 39.4°, confirming carbonate phase presence. Portlandite (4.8%) exhibited its most intense peak at 2θ = 18.1° with a secondary peak at 34.1°, representing typical Portland cement hydration products.

In Group 2, the optimized SCC–15%FGP + 5%SS + 1%FP mixture showed mainly crystalline structure dominated by quartz as the widespread mineral phase, comprising 91.7% of the total composition. The XRD analysis revealed the characteristic quartz diffraction pattern with the strongest peak at 2θ = 26.6°, accompanied by secondary peaks at 2θ = 20.8°, 39.4°, and 50.6°, confirming extensive residual crystalline silica content. The first detectable peak at 2θ = 18.04° corresponded to portlandite, with a maximum secondary portlandite peak at 2θ = 34.10°, indicating limited unreacted calcium hydroxide presence. Additionally, calcite constituted 4.3% of the mixture with its diagnostic peak at 2θ = 29.4°, Indicating effective calcium consumption in C–S–H gel formation rather than carbonate precipitation, thereby confirming enhanced pozzolanic reactivity attributed to the fine particle size of FGP and high silica slurry reactivity.

In Group 3 (Fig. 13c), the SCC–15%CGP mixture showed a crystalline structure primarily dominated by calcite (54.4%), as revealed by the most intensive peak at 2θ = 29.4°, along with secondary reflections at 2θ = 23.0°, 43.1°, and 48.5°, pointing to increased calcium carbonate precipitation. Quartz, accounting for 23.7% of the crystalline phases, was identified with its most intensive peak at 2θ = 20.4°, and a secondary peak at 2θ = 26.1°, indicating persistent nonreactive silica due to the coarse particle size of CGP, which limits dissolution and pozzolanic interaction. Portlandite appeared at 21.8%, with its most intensive reflection at 2θ = 34.1°, and a secondary peak at 2θ = 50.8°, suggesting incomplete pozzolanic consumption of calcium hydroxide. Comparatively high portlandite content confirms that the coarse particle size reduced surface reactivity and limited C–S–H gel formation, resulting in a phase composition dominated by stable crystalline minerals, thereby demonstrating the low pozzolanic efficiency of CGP in its coarse form.

3.3.4 Porosity and surface area

The Multipoint BET Surface Area and Total Pore Volume Analysis performed on Self-Compacting Concrete (SCC) mixtures indicated significant insights into their porosity characteristics, as shown in Table 4 and described through adsorption–desorption isotherms in Fig. 14(a-c). The control mixture (S-CL) exhibited a baseline BET surface area of 353.41 m^2/g and total pore volume of 1.46 cm^3/g, with adsorption volumes of 180, 230, and 945 cm^3/g at relative pressures (P/P_0) of 0.4, 0.6, and 0.99 respectively, indicating a well-balanced pore structure. The hybrid mixture (Group 2—S-FGP15% + SS5% + FP1%) Including fine glass powder, silica slurry, and polyolefin fibers showed an increased BET surface area of 392.98 m^2/g and total pore volume of 1.55 cm^3/g, with associated adsorption volumes of 170, 220, and 1000 cm^3/g. This higher porosity, despite the inclusion of fine materials, was attributed to the polyolefin fibers creating interfacial transition zones (ITZ) that formed a

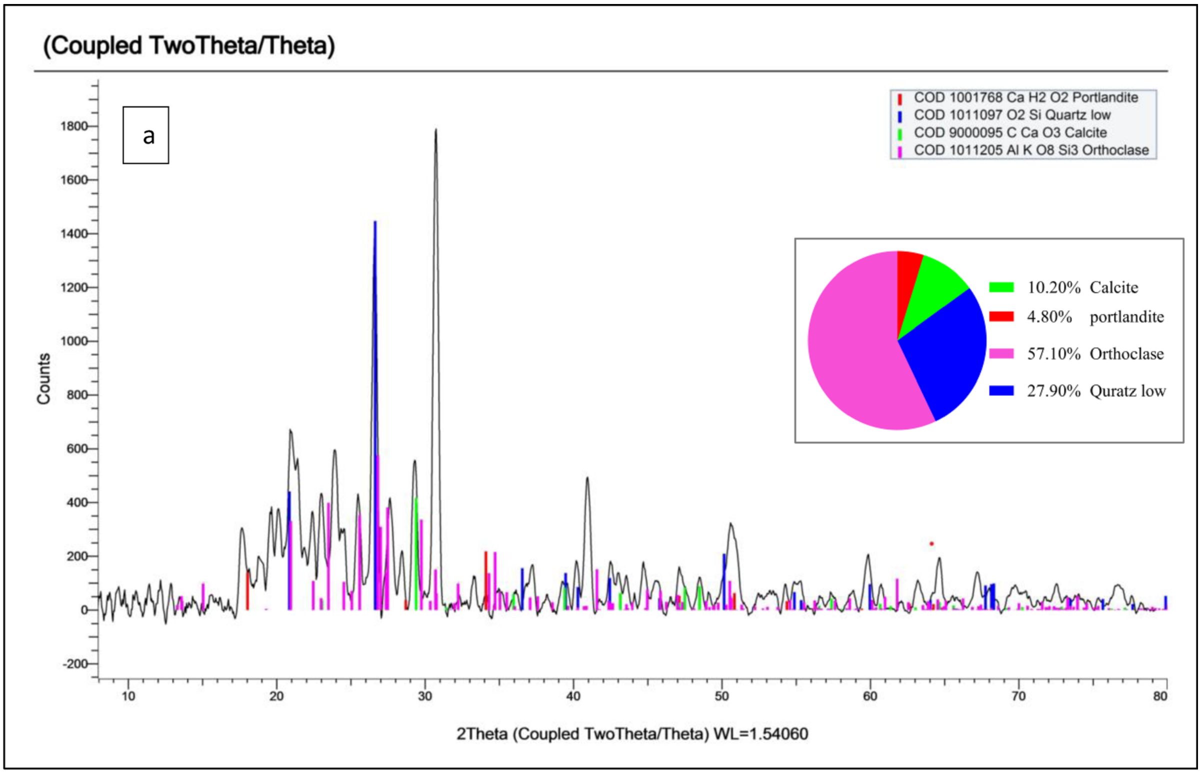

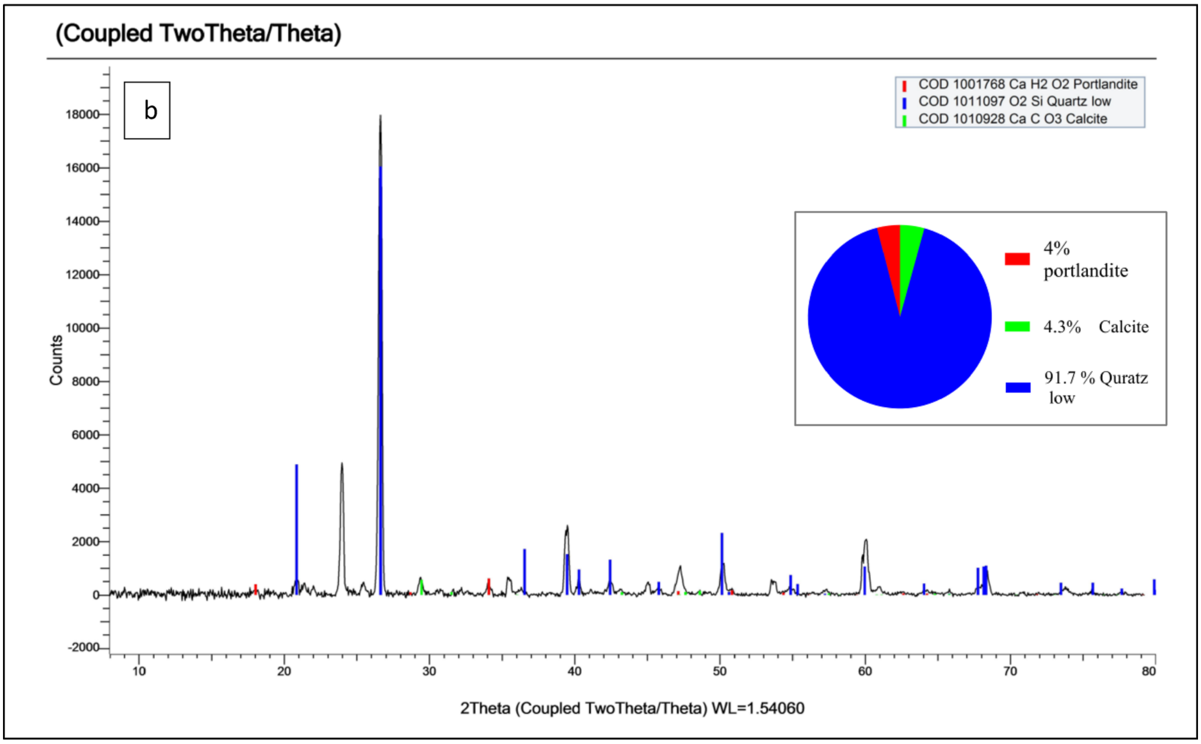

Fig. 13 X-ray diffraction (XRD) patterns and phase composition of concrete mixtures with various supplementary cementitious materials: (**a**) Control mixture, (**b**) combined fine glass powder and silica slurry + fiber polyolefin (SCC-15%FGP + 5%SS + 1%FP) mixture, (**c**) coarse glass powder (SCC-15%CGP) mixture

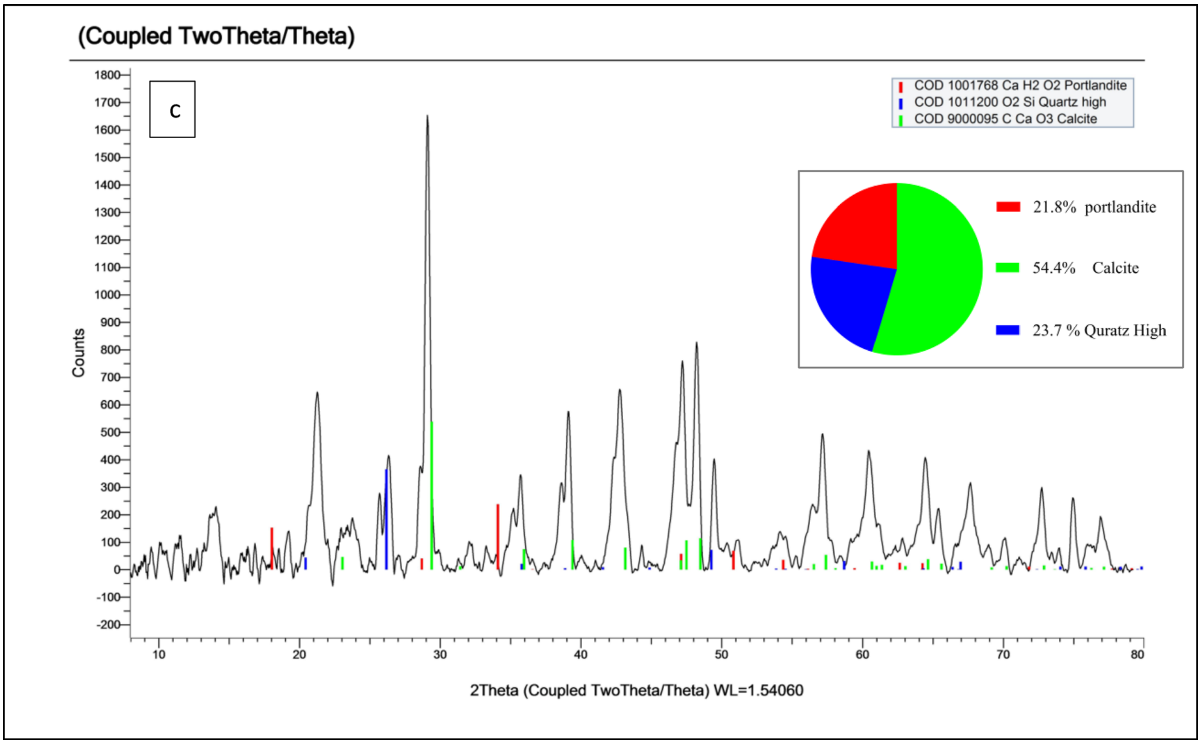

Fig. 13 (continued)

Table 4 Porosity Characteristics of Concrete Mixtures

Sample (code)	Multipoint BET surface area	Total pore volume
S-CL	353.41 m^2/g	1.46 cc/g
Group 2 S-FGP15% + SS5% + FP1%	392.98 m^2/g	1.55 cc/g
Group 3-S- CGP 15%	36.61 m^2/g	0.146 cc/g

network of microscopic channels. The water absorption results support this finding, showing that these channels enabled slightly increased water ingress despite the matrix densification supplied by the fine materials. Most notably, the coarse glass powder mixture (Group 3—S-CGP15%) showed remarkably reduced porosity characteristics, with BET surface area dropping to 36.61 m^2/g and total pore volume to 0.146 cm^3/g, while adsorption volumes decreased to 20, 25, and 100 cm^3/g respectively. This substantial reduction in porosity correlates perfectly with its superior water absorption resistance, providing strong evidence that coarse glass particles effectively block water penetration pathways by filling large pores and creating tortuous paths. The consistency between porosity measurements and water absorption performance validates the enhanced water resistance mechanisms of this mixture, though the reduced porosity may affect mechanical properties due to observed microstructural characteristics. These comprehensive findings across multiple testing methodologies demonstrate the complex relationship between pore structure and durability performance in SCC systems. These findings highlight a crucial observation: while the incorporation of fine materials in Group 2 was intended to enhance the concrete's density, the presence of organic polyolefin fibers created interfacial transition zones that unexpectedly increased porosity and water absorption. In developing contrast,

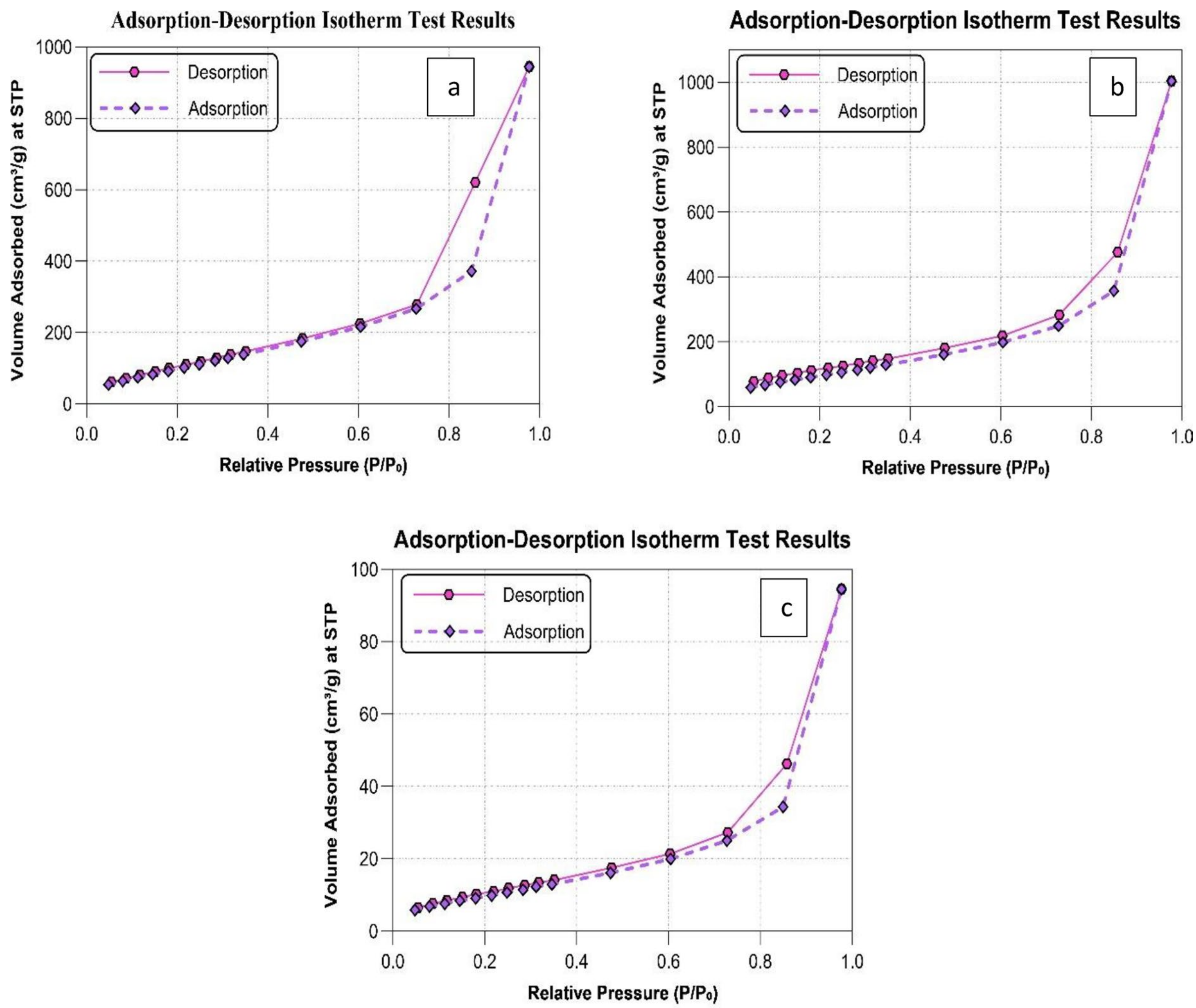

Fig. 14 Adsorption–Desorption Isotherms of Various Self-Compacting Concrete (SCC) Mixtures: (**a**) Control mixture, (**b**) Combined fine glass powder and silica slurry + fiber polyolefin (SCC-15%FGP + 5%SS + 1%FP) mixture, (**c**) coarse glass powder (SCC-15%CGP) mixture

the Group 3 mixture with coarse glass powder was found to be the most effective in enhancing concrete durability, successfully reducing porosity and water absorption by its unique characteristic of filling large pores and creating complex pathways that highly resist water movement within the concrete matrix.

4 Environmental impact and cost analysis

Glass Powder (coarse CGP and fine FGP), Silica Slurry, and Polyolefin Fibers are innovative materials that improve Self-Compacting Concrete (SCC) performance, sustainability, and economy. FGP, with high grinding, has greater pozzolanic activity with up to 45.24% increase in compressive strength at 15% replacement, while less reactive CGP is adequate performance at lower cost ($0.90/kg as opposed to FGP's $1.45/kg). Both reduce the use of sand by 15–20%, reducing the environmental impact, with FGP also exhibiting increased matrix densification with decreasing particle size. While more expensive to manufacture, both are economical relative to waste disposal costs, especially where landfills for glass waste are expensive CGP is appropriate for medium strength applications required, while FGP is suitable for high-strength, long-term high-performance concrete. Silica Slurry can be used as an economic replacement for cement (up to 10%) reducing the consumption of Portland cement while lowering construction carbon footprint. It is a rheological property improvement for SCC, which is workable without segregating and without excess water and admixtures, having improved cohesion. At a cost of $0.80/liter, it is an economical solution that improves both performance and sustainability. Polyolefin Fibers are a cheap alternative to steel fibers ($1.00/kg vs. $4.00-$5.00/kg) with enhanced tensile and flexural strength, enhanced ductility, and mixed integrity at 1% addition by weight. Together, these materials make high-performance concrete with improved durability, reduced cost, and reduced environmental impact reality.

5 Conclusion

This research illustrates the complex interaction among fine glass powder (FGP), coarse glass powder (CGP), silica slurry (SS), and synthetic polyolefin fibers (PF) in the matrix of modern self-compacting concrete (SCC). Following a systematic experimental approach, optimum ratios were determined to obtain a combination of 15% FGP, 5% SS, and 1% PF—termed Mix S-FGL15% + SL5% + FP1% for synergistic improvement in both fresh and hardened properties of concrete.

In their fresh state, polyolefin fibers were highly effective in mitigating segregation risks due to their high fine content. The optimum dosage of 1% fiber brought the GTM segregation index to its minimum value in the Mix S-GL15% + SL5% + FP1%, ensuring stability when added. The round shape of FGP improved greatly the flowability, allowing an increase of 17% in slump flow with maintained passing ability (L-box ratio > 0.8). Silica slurry complemented these improvements through its lubricating effect, creating a highly stable and workable matrix. On the contrary, CGP being angular in shape was used in Mix S-CG15% and increased internal friction, which affected workability. This latter characteristic, however, would also improve mechanical interlocking and segregation resistance, proving that CGP is effective as a stabilizer for mixes with high flowability demands.

The mechanical properties showed excellent improvement in several respects. The long-term performance was very important for FGP, where compressive strength at 90 days showed an increase of 45.24% in Mix S-FGL15% + SL5% + FP1% due to continuous pozzolanic reactivity and better particle packing. In addition, XRD confirmed the increased formation of the C-S–H gel resulting from the interaction of FGP with cement hydrates; SS further improved the development of early-age strength, showing an increase of 25.79% in tensile strength at 28 days. Flexural strength showed an increase of 80.75%, which is due to the micro-filling effect of SS and the crack-bridging capabilities of PF. Coarse glass powder was a cost-effective alternative in Mix S-CGP 15%, as its larger particle size required minimal processing. Although it caused a slight reduction in compressive strength, by 4.76% at 90 days, it brought about high-cost advantages and increased interlocking effects, which made it appropriate for structural applications where the economy is preferred over peak mechanical performance.

Durability-related properties were considerably improved. The best combination, Mix S-FGP15% + SS5% + FP1%, had a 35.7% decrease in sorptivity, indicating higher surface water resistance. This improvement can be largely attributed to the effect of pore refinement by fine materials. Total water absorption tests, however, indicated a marginal increase of 2.56%, with a rise in BET surface area from 353.41 m^2/g to 392.98 m^2/g and total pore volume from 1.46 cm^3/g to 1.55 cm^3/g. Such apparent contradiction can be explained due to the formation of interfacial transition zones (ITZ) induced by polyolefin fibers. These ITZ, while creating microscopic channels that slightly increased the total porosity, contributed significantly to stress distribution and crack resistance mechanisms, as confirmed through detailed microstructural analysis using SEM and stereomicroscopic techniques. Besides, the CGP component was highly effective in Mix S-CGP5%, significantly enhancing water resistance by filling larger pores—a critical property for applications that need to be of greater lower permeability. These results definitively establish superior durability.

This paper is a significant contribution to SCC technology, as it develops strong relationships between the proportions of the materials and the performance of SCC. The addition of FGL and SS for improving hydration kinetics, PF for enhancing crack resistance, and CGP for economic and structural purposes, in this way, makes the study well-balanced in its approach toward optimization of SCC performance. Results of this nature provide valid grounds for developing high-performance concretes for diversified construction needs, considering technical excellence, economic viability, and environmental sustainability.

Funding Open access funding provided by The Science, Technology & Innovation Funding Authority (STDF) in cooperation with The Egyptian Knowledge Bank (EKB).

Data availability No datasets were generated or analyzed during the current study.

References

1. Kou SC, Poon CS (2009) Properties of self-compacting concrete prepared with recycled glass aggregate. Cem Concr Compos 31(2):107–113
2. Liu M (2011) Incorporating ground glass in self-compacting concrete. Constr Build Mater 25(2):919–925
3. Ibrahim KIM (2021) Recycled waste glass powder as a partial replacement of cement in concrete containing silica fume and fly ash. Case Stud Constr Mater 15:e00630
4. Adaway M, Wang Y (2015) Recycled glass as a partial replacement for fine aggregate in structural concrete-effects on compressive strength. Electron J Struct Eng 14(1):116–122
5. Khan AG, Khan B (2017) Effect of partial replacement of cement by mixture of glass powder and silica fume upon concrete strength. Int J Eng Works 4(7):124–135
6. Dobiszewska M, Pichór W, Tracz T, Petrella A, Notarnicola M (2023) Effect of Glass Powder on the Cement Hydration, Microstructure and Mechanical Properties of Mortar. Mater Proc 13:40. https://doi.org/10.3390/materproc2023013040
7. Ortega JM, Letelier V, Solas C, Miró M, Moriconi G, Climent MÁ, Sánchez I (2018) Influence of waste glass powder addition on the pore structure and service properties of cement mortars. Sustainability 10:842
8. Safarizki HA, Gunawan LI, Marwahyudi. (2020) Effectiveness of Glass Powder as a Partial Replacement of Sand in Concrete Mixtures. J Phys: Conf Series 1625:012025. https://doi.org/10.1088/1742-6596/1625/1/012025
9. Idir R, Cyr M, Tagnit-Hamou A (2011) Pozzolanic properties of fine and coarse color glass cullet. Cem Concr Compos 33(1):19–29
10. Aliabdo AA, Abd Elmoaty M, Aboshama AY (2016) Utilization of waste glass powder in the production of cement and concrete. Constr Build Mater 124:866–877
11. Fattouh MS, Elsayed EK (2023) Influence of utilizing glass powder with silica fume on mechanical properties and microstructure of concrete. Delta Univ Sci J 6(1):111–122
12. AboEl-Kassem MH, Mohamed OM, Abd El-Hamid MZ (2022) Effect of using glass powder as a partial replacement of cement on concrete properties. J Al-Azhar Univ Eng Sector JAUES 17(62):219–236
13. Yusuf MO, Al-Sodani KAA, AlAteah AH et al (2022) Performances of the synergy of silica fume and waste glass powder in ternary blended concrete. Appl Sci 12:6637
14. Tariq S, Scott AN, Mackechnie JR, Shah V (2020) The durability of high-volume glass powder self-compacting concrete. Appl Sci 10:8058
15. Safarizki HA, Gunawan Marwahyudi LI (2020) Effectiveness of glass powder as a partial replacement of sand in concrete mixtures. J Phys: Conf Series. 1625:012025
16. Said AM, Zeidan MS, Bassuoni MT, Tian Y (2012) Properties of concrete incorporating nano-silica. Constr Build Mater 36:838–844
17. Behnood A, Ziari H (2008) Effects of silica fume addition and water-to-cement ratio on the properties of high-strength concrete after exposure to high temperatures. Cem Concr Compos 30(2):106–112
18. Alberti MG, Enfedaque A, Gálvez JC (2014) On the mechanical properties and fracture behavior of polyolefin fiber-reinforced self-compacting concrete. Constr Build Mater 55:274–288
19. Pająk M, Ponikiewski T (2013) Flexural behavior of self-compacting concrete reinforced with different types of steel fibers. Constr Build Mater 47:397–408
20. Afroughsabet V, Ozbakkaloglu T (2015) Mechanical and durability properties of high-strength concrete containing steel and polypropylene fibers. Constr Build Mater 94:73–82
21. Cifuentes H, García F, Maeso O, Medina F (2013) Influence of the properties of polypropylene fibers on the

fracture behavior of low-, normal- and high-strength FRC. Constr Build Mater 45:130–137
22. Banthia N, Sappakittipakorn M (2007) Toughness enhancement in steel fiber reinforced concrete through fiber hybridization. Cem Concr Res 37(9):1366–1372
23. Adhikary SK, Rudzionis Z, Balakrishnan A, Jayakumar V (2019) Investigation on the mechanical properties and post-cracking behavior of polyolefin fiber reinforced concrete. Fibers 7:8
24. Behfarnia K, Behravan A (2014) Application of high-performance polypropylene fibers in concrete lining of water tunnels. Mater Des 55:274–279
25. Alberti MG, Enfedaque A, Gálvez JC, Agrawal V (2016) Reliability of polyolefin fiber reinforced concrete beyond laboratory sizes and construction procedures. Compos Struct 140:506–524
26. Smirnova O, Kharitonov A, Belentsov Y (2022) Influence of polyolefin fibers on the strength and deformability properties of road pavement concrete. J Traffic Transp Eng 6(4):407–417
27. Sabri I, Mahdi M, Ojaimi M (2022) Destructive and non-destructive tests formulation for concrete containing polyolefin fibers. Open Eng 12:760–768
28. CEN. (2019a). EN 12350–8: Testing fresh concrete - Part 8: Self-compacting concrete - Slump-flow test. European Committee for Standardization, Brussels, Belgium.
29. CEN. (2019b). EN 12350–12: Testing fresh concrete - Part 12: Self-compacting concrete - J-ring test. European Committee for Standardization, Brussels, Belgium.
30. CEN. (2019c). EN 12350–10: Testing fresh concrete - Part 10: Self-compacting concrete - L box test. European Committee for Standardization, Brussels, Belgium.
31. CEN. (2019d). EN 12350–11: Testing fresh concrete - Part 11: Self-compacting concrete - Sieve segregation test. European Committee for Standardization, Brussels, Belgium.
32. ASTM C1585–13 (Reapproved 2018): Standard Test Method for Measurement of Rate of Absorption of Water by Hydraulic Cement Concretes.
33. ASTM C642–21: Standard Test Method for Density, Absorption, and Voids in Hardened Concrete.